Peripapillary Retinal Pigment Epithelium Layer Shape Changes From Acetazolamide Treatment in the Idiopathic Intracranial Hypertension Treatment Trial

Jui-Kai Wang,[1] Randy H. Kardon,[2,3] Johannes Ledolter,[2,4] Patrick A. Sibony,[5] Mark J. Kupersmith,[6] and Mona K. Garvin[1,2]; for the OCT Sub-Study Committee and the NORDIC Idiopathic Intracranial Hypertension Study Group

[1]Department of Electrical and Computer Engineering, The University of Iowa, Iowa City, Iowa, United States
[2]Iowa City VA Health Care System and Iowa City VA Center for the Prevention and Treatment of Visual Loss, Iowa City, Iowa, United States
[3]Department of Ophthalmology and Visual Sciences, The University of Iowa, Iowa City, Iowa, United States
[4]Department of Management Sciences/Department of Statistics and Actuarial Science, The University of Iowa, Iowa City, Iowa, United States
[5]Department of Ophthalmology, University Hospital and Medical Center, SUNY Stony Brook, Stony Brook, New York, United States
[6]Icahn School of Medicine at Mount Sinai and New York Eye and Ear Infirmary, New York, New York, United States

Correspondence: Mona K. Garvin, 4318 Seamans Center for the Engineering Arts and Sciences, The University of Iowa, Iowa City, IA 52242, USA;
mona-garvin@uiowa.edu.

See the appendix for the members of for the OCT Sub-Study Committee and the NORDIC Idiopathic Intracranial Hypertension Study Group.

Submitted: November 9, 2016
Accepted: March 29, 2017

Citation: Wang J-K, Kardon RH, Ledolter J, Sibony PA, Kupersmith MJ, Garvin MK; for the OCT Sub-Study Committee and the NORDIC Idiopathic Intracranial Hypertension Study Group. Peripapillary retinal pigment epithelium layer shape changes from acetazolamide treatment in the idiopathic intracranial hypertension treatment trial. *Invest Ophthalmol Vis Sci*. 2017;58:2554–2565. DOI:10.1167/iovs.16-21089

Purpose. Recent studies indicate that the amount of deformation of the peripapillary retinal pigment epithelium and Bruch's membrane (pRPE/BM) toward or away from the vitreous may reflect acute changes in cerebrospinal fluid pressure. The study purpose is to determine if changes in optic-nerve-head (ONH) shape reflect a treatment effect (acetazolamide/placebo + weight management) using the optical coherence tomography (OCT) substudy of the Idiopathic Intracranial Hypertension Treatment Trial (IIHTT) at baseline, 3, and 6 months.

Methods. The pRPE/BM shape deformation was quantified and compared with ONH volume, peripapillary retinal nerve fiber layer (pRNFL), and total retinal (pTR) thicknesses in the acetazolamide group (39 subjects) and placebo group (31 subjects) at baseline, 3, and 6 months.

Results. Mean changes of the pRPE/BM shape measure were significant and in the positive direction (away from the vitreous) for the acetazolamide group ($P < 0.01$), but not for the placebo group. The three OCT measures reflecting the reduction of optic disc swelling were significant in both treatment groups but greater in the acetazolamide group ($P < 0.01$).

Conclusions. Change in the pRPE/BM shape away from the vitreous reflects the effect of acetazolamide + weight management in reducing the pressure differential between the intraocular and retrobulbar arachnoid space. Weight management alone was also associated with a decrease in optic nerve volume/edema but without a significant change in the pRPE/BM shape, implying an alternative mechanism for improvement in papilledema and axoplasmic flow, independent of a reduction in the pressure differential. (ClinicalTrials.gov number, NCT01003639.)

Keywords: papilledema, Bruch's membrane, optical coherence tomography, shape analysis, intracranial hypertension

Idiopathic intracranial hypertension (IIH) is a clinical syndrome that predominantly affects young overweight women. It is characterized by an elevated intracranial pressure (ICP), otherwise normal cerebrospinal fluid, headaches, pulsatile tinnitus, and papilledema. Imaging studies are usually normal but often show distension of the nerve sheaths, flattening of the globe, empty sella, and stenosis of the transverse sinuses.[1,2] Recently, a nationwide treatment trial of IIH, called the Idiopathic Intracranial Hypertension Treatment Trial (IIHTT), was completed; the IIHTT was a multicenter, randomized, double-masked, placebo-controlled clinical trial that demonstrated the effectiveness of acetazolamide + weight management versus placebo + weight management for improving the visual field and quality of life in treatment of 165 patients with IIH and mild vision loss.[3–5] The optical coherence tomography (OCT) substudy was further designed to explore continuous-scale structural parameters to quantitatively monitor the changes over time in the optic nerve head (ONH) and macular regions using spectral-domain OCT (SD-OCT) images.[6–8] The preliminary outcomes from the IIHTT OCT substudy showed that the standard OCT measures of papilledema (including the ONH volume, mean peripapillary retinal nerve fiber layer [pRNFL] and total retinal [pTR] thicknesses) were reliable and responsive to the effects of acetazolamide on papilledema.[6–8]

In addition to the standard OCT measures that have been introduced in the previous paragraph, our group recently reported that the shape of the peripapillary retinal pigment epithelium and/or Bruch's membrane (pRPE/BM) layer in

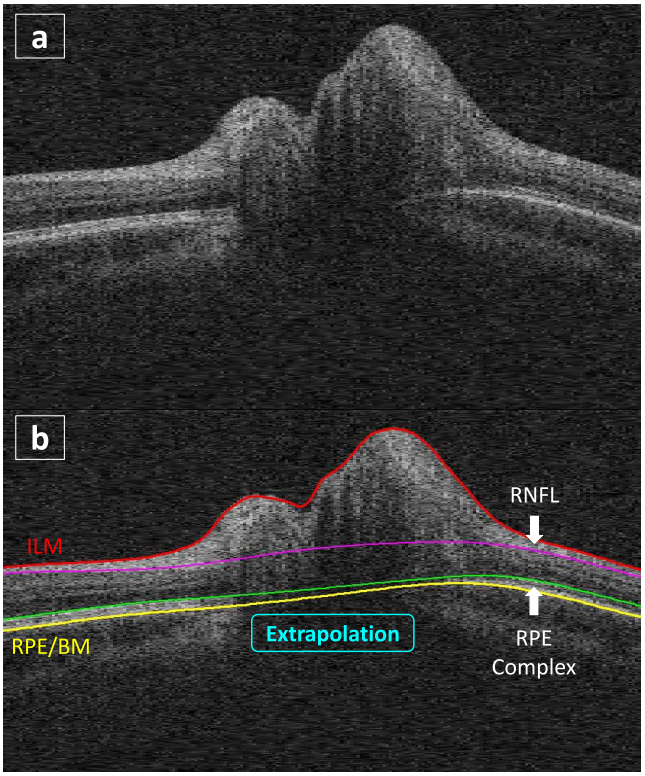

Figure 1. Example of 3D retinal layer segmentations in SD-OCT images. (**a**) The central B-scan of an ONH scan. (**b**) Layer segmentation in the ONH scan.

patients with intracranial hypertension (ICH) is displaced anteriorly toward the vitreous, and this shape difference is not otherwise explained by disc edema alone.[9,10] It has been shown that interventions that lower the ICP (e.g., spinal tap, shunting procedure, or medical treatment of IIH) will normalize the anterior displaced pRPE/BM layer in a posterior direction away from the vitreous.[11] In the original method of generating the pRPE/BM shape model, 10 equidistant landmarks were manually placed from the pRPE/BM opening (BMO) along the pRPE/BM boundary at both nasal and temporal directions in the central high-definition 5-line raster (HD-5LR) B-scan for each available subject.[10] However, this manual procedure is very time consuming. Therefore, we further developed a semiautomated methodology[12] to more efficiently place the landmarks on the pRPE/BM surface to make the pRPE/BM shape model available in larger data sets (also see Methods).

The relationships among the standard OCT measures reflecting ONH swelling and clinical features at baseline, 3-, and 6-month time points under treatment with either acetazolamide + weight management or placebo + weight management were previously reported in the IIHTT OCT substudy.[6–8] However, details about how the pRPE/BM shape prospectively changes in response to therapy in these cohorts have not been reported. The purpose of this work was to (1) quantify the pRPE/BM shape deformation for all the available subjects in the longitudinal IIHTT OCT substudy with data of adequate quality for every scheduled visit, and (2) compare the newly computed pRPE/BM shape measure to the standard OCT measures of papilledema from baseline to 3 and to 6 months in both treatment groups. A semiautomated method[12] was used to compute the pRPE/BM shape measure for each available subject in the IIHTT OCT substudy data set at presentation as well as at follow-up points during the study treatment interval

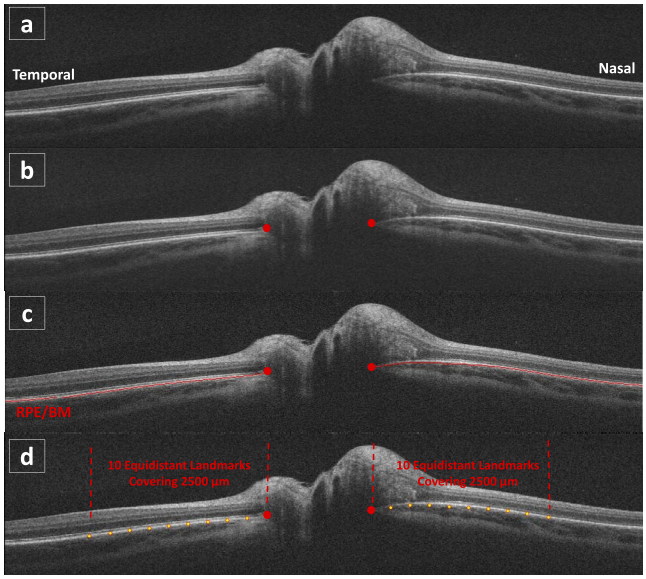

Figure 2. Steps of semiautomated landmark placement. (**a**) A central B-scan of a HD-5LR scan. (**b**) Manual BMO landmark placement. (**c**) Automated 2D layer segmentation. (**d**) The pRPE/BM shape comprising of the manual (*the red dots*) and semiautomated (*the yellow dots*) landmarks.

for 6 months to determine whether the pRPR/BM shape change reflects a treatment effect.

Methods

Data Acquisition

Clinical reports of the IIHTT were recently published,[3–5,13,14] and the OCT substudy outcomes were also released.[6–8] In IIHTT, the enrolled study eyes were from the worse eyes of the IIH patients naïve to treatments with a perimetric mean deviation (PMD) of −2.00 to −7.00 dB using the SITA standard 24-2 test pattern on the Humphrey Field Analyzer II perimeter (Swedish Interactive Threshold Algorithm; Carl Zeiss Meditec, Inc., Dublin, CA, USA).[3,5] In the IIHTT OCT substudy, 125 subjects were included at 24 sites[6–8] based on availability of OCT at the different study sites. Three SD-OCT image protocols were included in the OCT substudy: (1) the ONH-centered HD-5LR scan, (2) the volumetric ONH-centered scan, and (3) the volumetric fovea-centered macular scan (using the Cirrus 4000 SD-OCT machine with software version 6.01, Carl Zeiss Meditec, Inc.). All the OCT images for each subject were acquired from both eyes at the time points of baseline, 3-, and 6-month follow-up in both acetazolamide + weight management group and placebo + weight management groups. In this report, only accurately ONH-centered HD-5LR and volumetric scans with signal strength seven or greater were included.

Calculations of Conventional SD-OCT Parameters

As reported in our previous IIHTT OCT substudy baseline[6] and 6-month outcome papers,[8] commercial software for segmenting retinal layers in the ONH-centered OCT volumes had noticeably higher failure rates than the Iowa 3D graph-theoretical methods[15–18] when the optic disc was swollen. Therefore, in this work, only the Iowa 3D methods were used to automatically segment retinal layers (Fig. 1). Consistent with the methodology of the other IIHTT OCT substudy papers,[6,8] the ONH volume, mean pRNFL, and pTR thicknesses along a

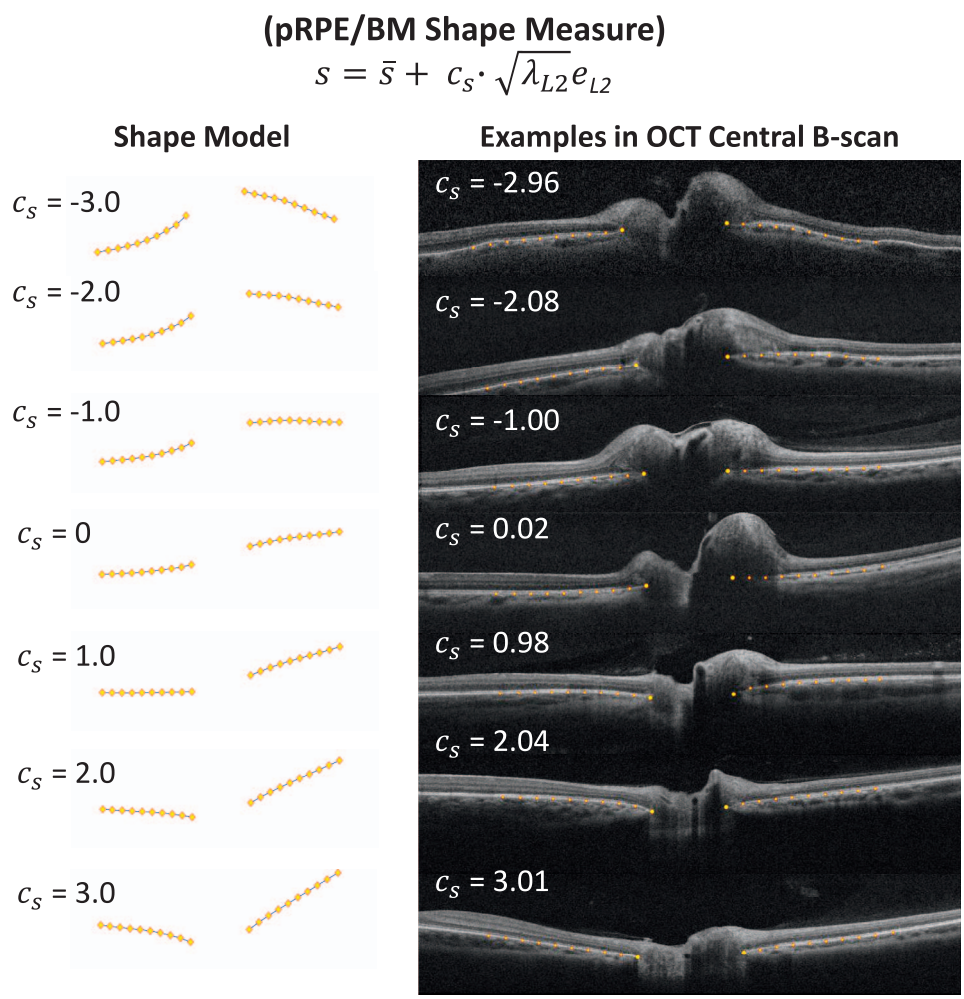

Figure 3. Statistical pRPE/BM shape model, which was generated by 116 baseline right eyes from the data set of IIHTT OCT substudy, where S, $\bar{S}$, λ_{L2}, e_{L2}, and c_s represent the pRPE/BM shape, the mean shape, the second largest eigenvalue (λ_{L2}), the eigenvector corresponding to λ_{L2} and the pRPE/BM shape measure, respectively. The *left column* shows the shape model changing with varying shape measure (c_s), and the *right column* shows example pRPE/BM shapes in the HD-5LR central B-scans.

radius of 1.73 mm around the center of the ONH were computed.[6,8]

Peripapillary RPE/BM Shape Deformation Measure From HD-5LR Scans

To quantify the pRPE/BM shape deformation, the pRPE/BM shape model was first generated. The traditional method[10] used 10 manual equidistant landmarks starting from the BMO along the pRPE/BM boundary covering 2.5 mm in length at each nasal and temporal side in the HD-5LR OCT central B-scan, which passes through the center of the optic disc. Therefore, the pRPE/BM shape derived from the central B-scan contained 20 equidistant landmarks. However, manual placement of 20 equidistant landmarks in OCT B-scans in a large data set requires a lengthy manual processing time and very specific expertise, making the originally reported shape analysis[10] difficult to perform in the large IIHTT data set, motivating the present semiautomated analysis.

In this work, a custom semiautomated method[12] (Fig. 2) was used to accelerate the process of sampling landmarks used in the previous work.[10] Two landmarks were first manually placed at the end of the BM surface in the central HD-5LR B-scan (the red dots in Fig. 2b), and then the complete pRPE/BM surface was automatically segmented using a graph-based algorithm[15,18] (i.e., the red line in Fig. 2c). Then the other 18 equidistant landmarks were automatically placed along the presegmented pRPE/BM surface covering 2.5 mm at both nasal and temporal side (the yellow dots in Fig. 2d). In particular, during the process of manually placing the two BMO landmarks, only the information from the image itself was used; no subject information, such as treatment group labels, ICP measures, subject visit labels, was considered.

Applying the process of landmark placing to 116 available baseline right eyes from the IIHTT OCT substudy data set, Procrustes analysis and principal component analysis (PCA) were used to generate the pRPE/BM shape models.[12] In addition, the scaling step in Procrustes analysis was particularly excluded to preserve the meaningful distances among the landmarks, which are defined based on physical distances along the pRPE/BM surface from the BMO. As previously demonstrated,[12] the second principal component of the pRPE/BM shape models, called the pRPE/BM shape measure (c_s) in this work, represents the degree of the pRPE/BM anterior/posterior displacement, which means that a more negative value of the coefficient reflects a larger pRPE/BM displacement toward the vitreous and vice versa (Fig. 3). Next, the pRPE/BM shape measure was computed for each available subject at

Investigative Ophthalmology & Visual Science

Table 1. OCT Scan Distributions in the Acetazolamide and Placebo Groups at Three Different Time Points (Considering Study Eyes Only)

	HD Raster Scan				ONH-Centered Scan			
Scan Type	**Baseline, *n* (%)**	**Month 3, *n* (%)**	**Month 6, *n* (%)**	**Intersection, *n* (%)**	**Baseline, *n* (%)**	**Month 3, *n* (%)**	**Month 6, *n* (%)**	**Intersection, *n* (%)**
Acetazolamide group								
Good scan	58 (93.6)	43 (69.4)	47 (75.8)	39 (62.9)	60 (96.8)	46 (74.2)	48 (77.4)	42 (67.7)
Missing scan	1 (1.6)	15 (24.2)	14 (22.6)		0 (0)	15 (24.2)	14 (22.6)	
Bad scan	2 (3.2)	1 (1.6)	0 (0)		2 (3.2)	1 (1.6)	0 (0)	
Wrong scan	1 (1.6)	3 (4.8)	1 (1.6)		0 (0)	0 (0)	0 (0)	
Total	62	62	62		62	62	62	
Total of available subjects in the acetazolamide group: 39 ∩ 42 = 39 (62.9)								
Placebo group								
Good scan	59 (93.7)	41 (65.1)	40 (63.5)	34 (54.0)	60 (95.2)	44 (69.8)	40 (63.5)	36 (57.1)
Missing scan	1 (1.6)	19 (30.2)	20 (31.8)		1 (1.6)	19 (30.2)	20 (31.8)	
Bad scan	0 (0)	2 (3.2)	0 (0)		2 (3.2)	0 (0)	3 (4.8)	
Wrong scan	3 (4.8)	1 (1.6)	3 (4.8)		0 (0)	0 (0)	0 (0)	
Total	63	63	63		63	63	63	
Total of available subjects in the placebo group: 34 ∩ 36 = 31 (49.2)								

Baseline, Month 3, and Month 6: The number of subjects having OCT images at baseline, 3 months, and 6 months, respectively. Intersection: the number of subjects having all baseline, 3-month, and 6-month OCT images available. Good scan: the number of subjects having available OCT scans to be correctly segmented and measured (at the given time point). Missing scan: the number of subjects having unavailable OCT scans due to the scan either not being acquired or not successfully converted from the proprietary image format to a format readable by our algorithms. Bad scan: the number of subjects having unavailable OCT scans due to bad image quality (severe motion artifacts, image center deviated from the ONH center, or random regions with extremely weak intensity). Wrong scan: the number of subjects having only fovea-centered HD-5LR scans rather than the required ONH-centered HD-5LR scans (only applicable to HD-5LR scans).

baseline, 3-, and 6-month follow-up visits in the IIHTT OCT substudy data set. Note that the method of computing the pRPE/BM shape measure had been previously validated in a subset of 20 scans covering the full shape change range through a comparison of the shape measures using the semiautomated approach with a fully manual approach (correlation: 0.99, $P < 0.01$) and comparison of the shape measures using the semiautomated approach with two different expert's manual markings of the BMO (correlation: 0.99, $P < 0.01$).[12]

Results

Data Distribution

Of the 125 subjects in the OCT substudy, 62 in the acetazolamide + weight management group (also referred to as the acetazolamide group) and 63 subjects in the placebo + weight management group (also referred to as the placebo group) had OCT data.[6–8] Only considering study eyes in this data set, Table 1 shows the reasons of the unavailable OCT scans in the acetazolamide and placebo groups at baseline, 3, and 6 months for both OCT HD-5LR and ONH-centered protocols. Three categories were typical. The "missing scans" were the cases in which these OCT images were either not acquired in the first place (mostly occurred at the 3- and/or 6-month visits) or not successfully converted from the proprietary image format to a format readable by our algorithms. "Bad scans" represent the OCT scans with bad image quality, so the layer segmentation algorithm failed to process them. Typical situations included: (1) the images had severe motion artifacts, (2) the centers of these images were off from the ONH center, or (3) the images had random regions with extremely low intensity. "Wrong scans" were only applicable for the HD-5LR scans. These scans were inaccurately acquired using macular protocol instead of the required ONH-centered protocol. To fairly compare the pRPE/BM shape measure with the other OCT measures (i.e., the pRNFL and pTR thicknesses, and the ONH volume) in both treatment groups at the baseline, 3, and 6-month follow-ups, the subjects who did not have complete measurements from both OCT image protocols and longitudinal time points were further excluded. The number of subjects with complete OCT measures at all three visits in the acetazolamide group and placebo group were 39/62 (62.9%) and 31/63 (49.2%), respectively; this data set will be referred to as the "complete data set" in the following sections. In addition, comparing the 70 subjects in the complete data set with the excluded 55 subjects, the unpaired *t*-tests failed to

Table 2. Repeated Measures ANOVAs for pRPE/BM Shape Measure, ONH Volume, pRNFL and pTR Thicknesses

	Treatment (DFn: 1, DFd: 68)		Time (DFn: 2, DFd: 136)		Treatment × Time (DFn: 2, DFd: 136)	
OCT Measures	***F* Value**	***P* Value**	***F* Value**	***P* Value**	***F* Value**	***P* Value**
pRPE/BM shape	3.44	0.07	9.74	< 0.01	7.48	< 0.01
ONHV	7.48	0.01	51.31	< 0.01	20.77	< 0.01
pRNFLT	3.19	0.08	32.45	< 0.01	13.19	< 0.01
pTRT	3.95	0.05	35.23	< 0.01	14.20	< 0.01

Includes nested random subject effects, fixed treatment effects, fixed time effects, and the interaction between treatment and time (treatment × time). DFd, degrees of freedom in the denominator; DFn, degrees of freedom in the numerator.

Investigative Ophthalmology & Visual Science

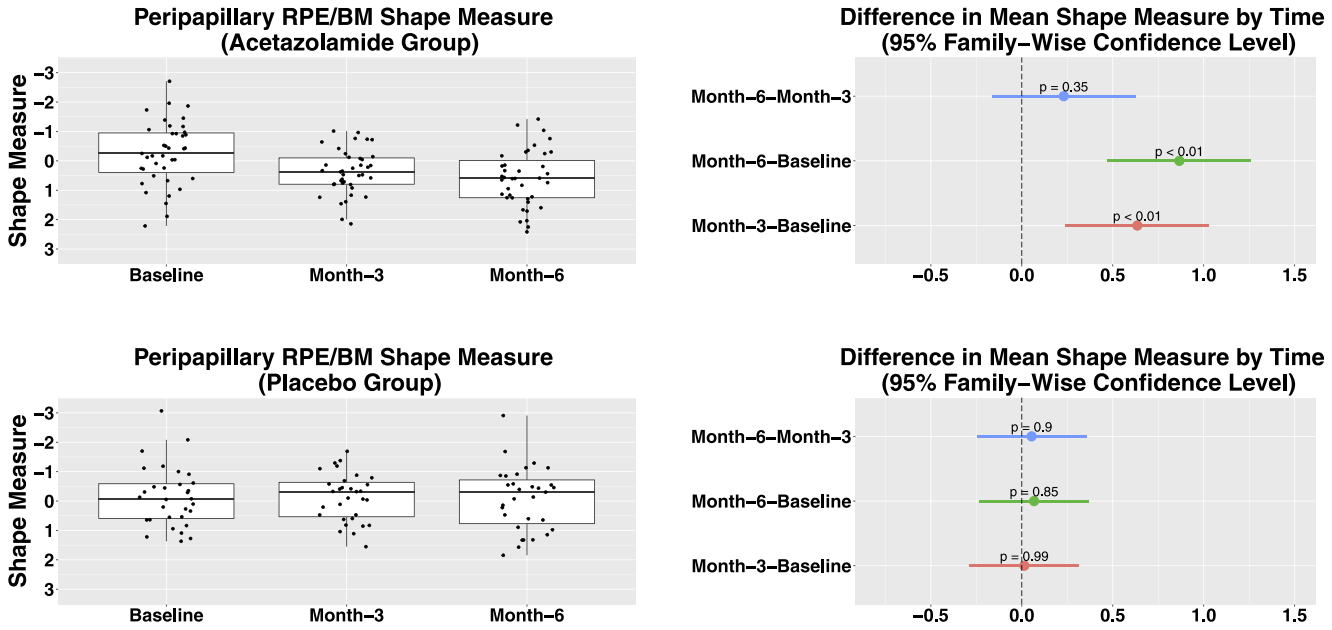

Figure 4. Box plots and Tukey pair-wise comparisons of the pRPE/BM shape measure in the acetazolamide group and placebo group.

show significant differences between both groups in PMD ($P = 0.64$) and in subject weights ($P = 0.66$), respectively.

Repeated Measures Analysis of Variance (ANOVA)

A repeated measures analysis of variance (using the ezANOVA[19] function in the R language) was applied for each OCT measure using a model with nested random subject effects (different subjects in each treatment group), fixed treatment effects (two treatment groups: acetazolamide and placebo), fixed time effects (three time visits: baseline, 3 months, and 6 months), and the interaction between treatment and time (treatment × time). Table 2 provides the *F*-values of each factor (treatment, time, and treatment × time) for each OCT measure and the associated probability values (*P* values). The ANOVA results indicate that the interactions between treatment and time (treatment × time) were significant for all the OCT measures ($P < 0.01$). Hence, the next steps were to assess (1) the effect of each treatment group on 3-month and 6-month changes from baseline, and (2) the effects of time, separately for each of the two study groups.

Table 3 shows the mean changes from baseline to 3- and to 6-month visit in both the acetazolamide group and placebo group. In the comparison of these two groups, the mean changes of the pRPE/BM shape measure from baseline to 3 and 6 months were both in the positive direction; this means the shape of pRPE/BM was oriented away from the vitreous. The mean shape change at 3 months (the value at 3 months minus that at baseline) was 0.64 vs. 0.01 and at 6 months (the value at 6 months minus that at baseline) was 0.87 vs. 0.07. The mean change of the ONH volume at 3 months was −4.21 vs. −0.35 mm^3 and at 6 months was −4.67 vs. −1.55 mm^3. The mean change of the pRNFL thickness at 3 months was −160.51 vs. −14.51 μm and at 6 months was −170.22 vs. −58.74 μm. The mean change of the pTR thickness at 3 months was −198.67 vs. −18.02 μm and at 6 months was −213.29 vs. −73.04 μm. One-sided two-sample (unpaired) *t*-tests were used to assess the significance of the differences between the mean changes in the acetazolamide and placebo groups. Differences for both 3-month and 6-month changes from baseline between these two groups were highly significant for all four outcome measures ($P < 0.01$). Mean changes of pRPE/BM shape measure from baseline were significantly more positive (i.e., away from the vitreous) in the acetazolamide group than the ones in the placebo group ($P < 0.01$). The results for the three conventional OCT measures also indicated that the reductions of the optic disc swelling were significantly greater in the

Table 3. OCT Measurements Changes With Acetazolamide/Placebo + Weight Management From Baseline to 3 and to 6 Months

OCT Measures	Treatment + Weight Loss	Baseline Mean	From 0 to 3 Months		From 0 to 6 Months	
			Mean Change	Standard Deviation	Mean Change	Standard Deviation
pRPE/BM Shape	Acetazolamide	−0.26	0.64	1.10	0.87	1.26
	Placebo	−0.14	0.01	0.73	0.07	0.75
ONHV, mm^3	Acetazolamide	16.30	−4.21	3.44	−4.67	3.76
	Placebo	15.36	−0.35	2.09	−1.55	2.48
pRNFLT, μm	Acetazolamide	274.65	−160.51	166.72	−170.22	174.14
	Placebo	225.36	−14.51	96.26	−58.74	117.38
pTRT, μm	Acetazolamide	534.49	−198.67	198.19	−213.29	207.82
	Placebo	478.28	−18.02	114.53	−73.04	139.59

In both periods, the changes in each OCT measure in the acetazolamide group were significantly different than the ones in the placebo group ($P < 0.01$, one-sided two-sample unpaired *t*-tests).

Investigative Ophthalmology & Visual Science

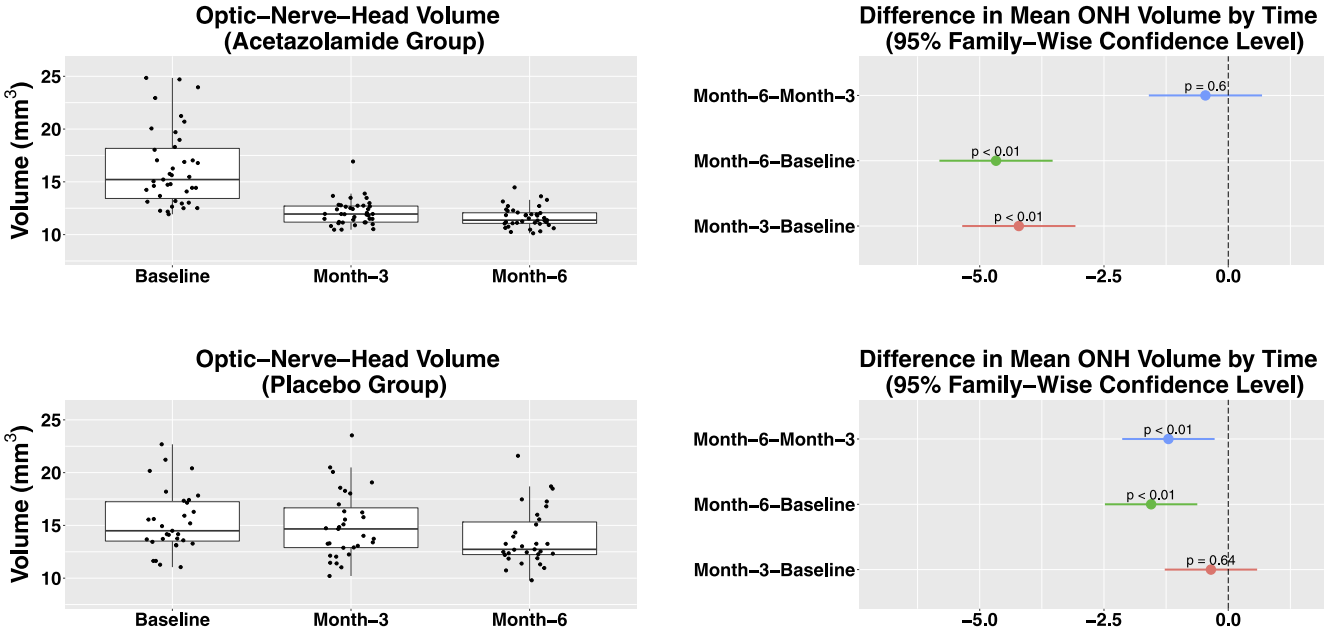

Figure 5. Box plots and Tukey pair-wise comparisons of the ONH volume in the acetazolamide group and placebo group.

acetazolamide group than the ones in the placebo group (all three P values < 0.01).

Box plots of the measurements at baseline, 3-month, and 6-month—shown separately for the two treatment groups—are given in Figures 4 through 7. A repeated measures ANOVA model with random subject effects and a fixed time effect were fit separately for the acetazolamide and the placebo group. The results in Table 4 show that the effect of time was significant for all cases (the two treatment groups and the four outcome measures), except for the pRPE/BM shape measure in the placebo group ($P = 0.85$).

Pairwise differences of average measurements at the three time periods (baseline, 3 months, and 6 months) are also shown in Figures 4 through 7, for both the acetazolamide group (top) and the placebo group (bottom). The 95% Tukey confidence intervals shown in these graphs adjust the overall error rate for all pairwise multiple comparisons and they use the error estimate from the repeated measures ANOVAs in Table 4. The Tukey confidence intervals for the acetazolamide and placebo groups are drawn on the same scale, to allow an assessment to the magnitude of the respective time effects.

In the acetazolamide group (top row in Fig. 4), the Tukey tests with 95% confidence level showed that the mean pRPE/BM shape measure changes from baseline were significantly more positive (away from vitreous) in 3 months and in 6 months ($P < 0.01$) but not from 3 to 6 months ($P = 0.35$). In the placebo group (bottom row in Fig. 4), the paired

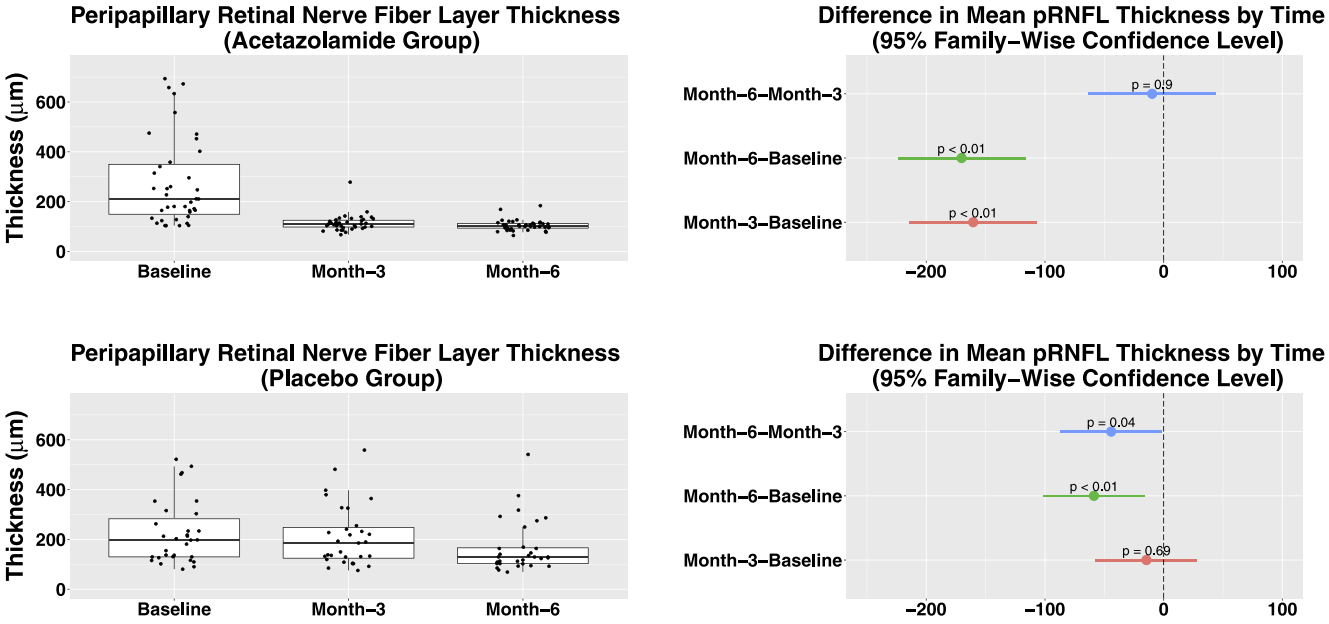

Figure 6. Box plots and Tukey pair-wise comparisons of the pRNFL thickness in the acetazolamide group and placebo group.

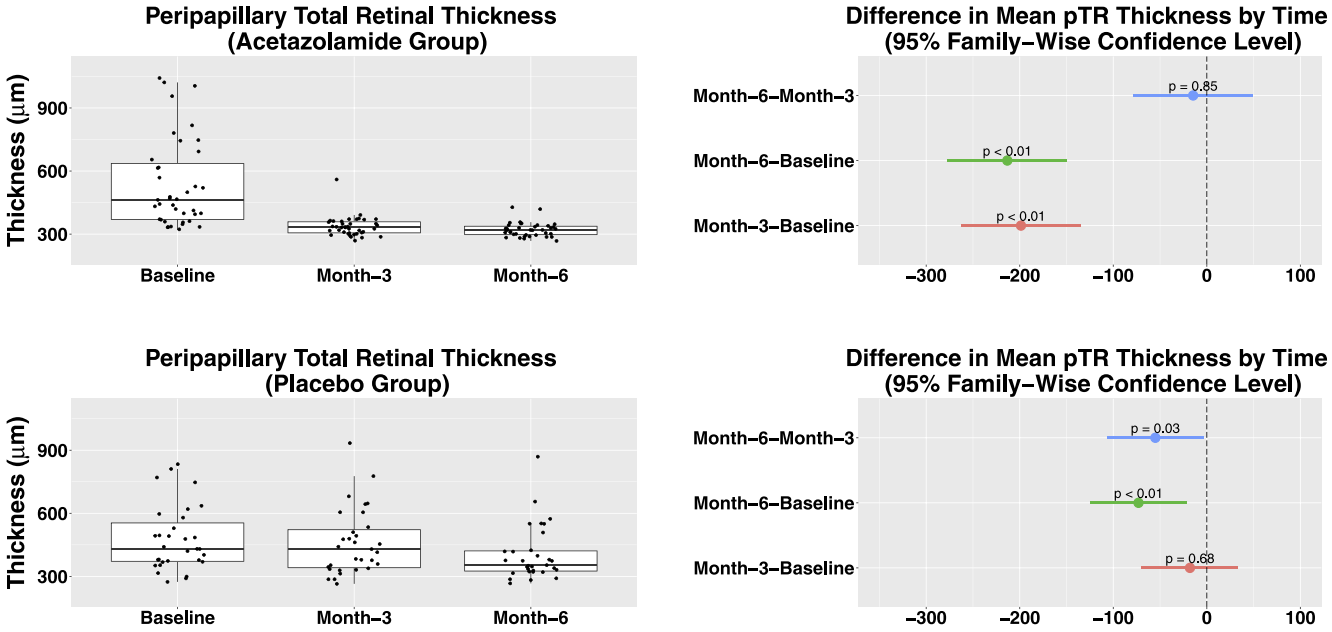

Figure 7. Box plots and Tukey pair-wise comparisons of the pTR thickness in the acetazolamide group and placebo group.

comparisons of the mean change of the shape measures were not significant among all three time periods ($P \geq 0.85$). For the other OCT measures (i.e., the ONH volume, pRNFL, and pTR thicknesses), in the acetazolamide group (top rows in Figs. 5, 6, 7), the significant changes also happened from baseline to 3 months and to 6 months ($P < 0.01$) but not from the 3 to 6 months ($P > 0.60$); in the placebo group (bottom rows in Figs. 5, 6, 7), the significant changes happened at least 3 months after baseline ($P < 0.01$).

Comparisons Between Groups With Positive and Negative Shape Change at 6 Months

Profile plots in Figure 8 illustrate the changes in the OCT measurements at baseline, 3, and 6 months in the acetazolamide (left column) and placebo (right column) groups. First, in Figure 8a, subjects were separated into two groups based on the pRPE/BM shape measure changes in 6 months: the cases with the pRPE/BM shape change toward vitreous in the top row; the cases with the shape change away from vitreous in the bottom row. Then, the same subject distribution setting was applied to the subfigures of the ONH volume, pRNFL, and pTR thicknesses (i.e., Figs. 8b, 8c, 8d). The median values of all the measurements at each time point in different groups were marked as black triangles. To visualize the ranges of normal subjects in these measurements, the numbers of the 5%, 50%, and 95% percentiles of 159 normal eyes were shown as the blue horizontal dot lines (Note: an independent data set was provided by Carl Zeiss Meditec, Inc.; subject ages $\leq$ 50). Particularly, comparing the cases in the acetazolamide group with positive pRPE/BM shape changes to the cases in the placebo group (i.e., the bottom rows in Figs. 8b, 8c, 8d), all three measurements show their median values were in the normal ranges after 3 months in the acetazolamide group, but similar progress in the placebo group needed to take 6 months.

Table 4. Results of the Repeated Measures ANOVAs

	Treatment + Weight Loss Group			
	Acetazolamide (DFn: 2, DFd: 76)		Placebo (DFn: 2, DFd: 60)	
OCT Measures	*F* Value	*P* Value	*F* Value	*P* Value
pRPE/BM shape	14.69	< 0.01	0.16	0.85
ONHV	58.44	< 0.01	8.87	< 0.01
pRNFLT	36.45	< 0.01	5.92	< 0.01
pTRT	39.82	< 0.01	6.26	< 0.01

Separated by treatment groups, with nested random subject effects plus a fixed time effect (baseline, 3 months, and 6 months). DFd, degrees of freedom in the denominator; DFn, degrees of freedom in the numerator.

Table 5. Pearson Correlations and Their *P* Values Between 3-Month (and 6-Month) Changes From Baseline of the pRPE/BM Shape Measure and 3-Month (and 6-Month) Changes of the Other OCT Measures (ONH Volume, pRNFL, and pTR Thicknesses)

Pearson Correlation (95% Confidence Level)	Change From Baseline to 3 Months		Change From Baseline to 6 Months	
	ρ	*P* Value	*ρ*	*P* Value
Shape vs. ONHV				
Acetazolamide, $n = 39$	−0.26	0.06	−0.28	0.04
Placebo, $n = 31$	−0.20	0.14	−0.22	0.12
Overall, $n = 70$	−0.37	< 0.01	−0.38	< 0.01
Shape vs. pRNFLT				
Acetazolamide, $n = 39$	−0.24	0.07	−0.26	0.06
Placebo, $n = 31$	−0.18	0.16	−0.13	0.25
Overall, $n = 70$	−0.33	< 0.01	−0.32	< 0.01
Shape vs. pTRT				
Acetazolamide, $n = 39$	−0.26	0.06	−0.26	0.05
Placebo, $n = 31$	−0.15	0.22	−0.12	0.26
Overall, $n = 70$	−0.34	< 0.01	−0.33	< 0.01

Correlations are shown for subjects in the acetazolamide group, for subjects in the placebo group, and for combined (overall).

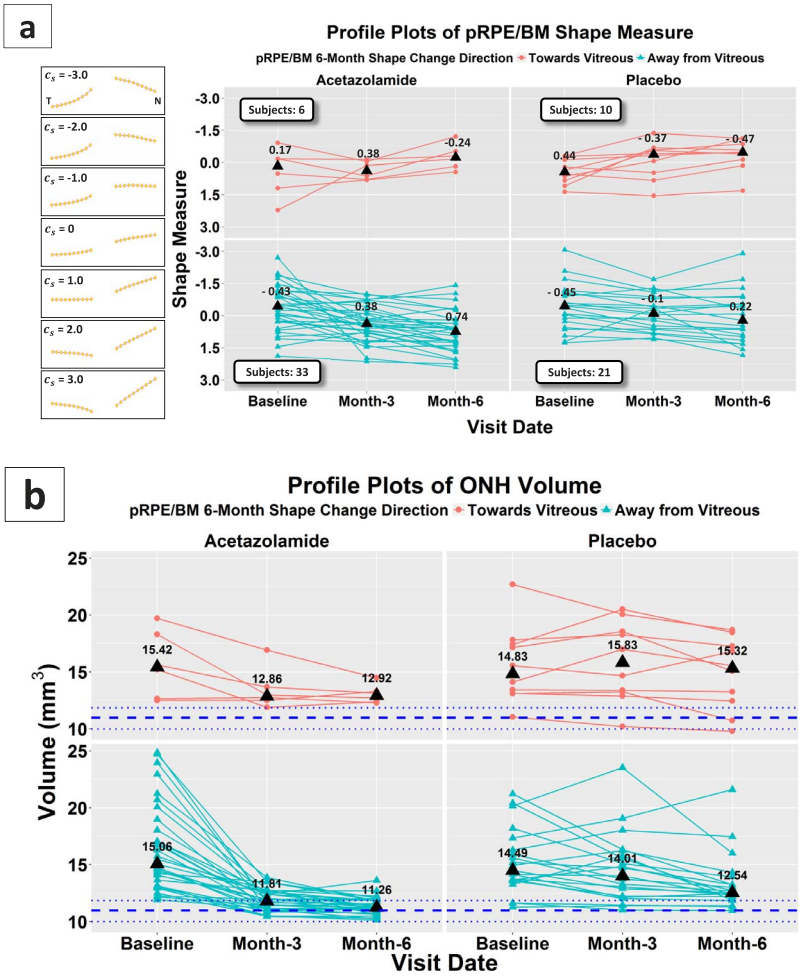

Figure 8. Profile plots for the OCT measures of the pRPE/BM shape measures, ONH volumes, pRNFL, and pTR thicknesses at baseline, 3 months, and 6 months for (1) subjects in the acetazolamide group (*left column*) and the placebo group (*right column*) and (2) subjects with 6-month pRPE/BM shape change toward vitreous (*top row*) and away from vitreous (*bottom row*). The *black triangles* represent the median values of each time point in different divisions, and the *blue horizontal lines* represent the 5%, 50% and 95% percentiles in 159 normal eyes (age $\leq$ 50 years).

Correlations Among Shape Measure and the Other OCT Measures

Pearson correlation tests (95% confidence level) were performed in the acetazolamide group (39 subjects), placebo group (31 subjects), and the overall group (total of 39 + 31 subjects) between 3-month (and 6-month) changes from baseline for the pRPE/BM shape measure and the other three OCT measures (Table 5). When separated by treatment groups, the correlation coefficients among changes in the shape measure and changes in the other OCT measures were small ($\rho \leq 0.28$) and insignificant ($P \geq 0.01$), for both 3-month and 6-month differences from baseline. Correlations reached a moderate level when all the subjects were combined ($-0.38 \leq \rho \leq -0.32$), with P values < 0.01.

Discussion

Our data show that normalization of the pRPE/BM shape, demonstrated by a semiautomated method of analysis of transaxial ONH images, reliably reflects the effect of acetazolamide + weight management in significantly improving the structural abnormalities associated with papilledema beyond the effects of weight management alone. Most of the change in shape of Bruch's membrane occurred during the 3 months of acetazolamide therapy, whereas no significant shape change occurred in the placebo group during the study period. Quantitative assessment of the pRPE/BM shape and subsequent change of the pRPE/BM shape appears to be another potential biomarker used to measure the success of treatment of raised ICP. The findings in this study are consistent with a previous study with similar findings after lowering the ICP using a different shape analysis methodology (Geometric Morphometrics)[11] and studies using various structural measures of the pRPE/BM surface.[20–22] Displacement of Bruch's membrane at the ONH appears to reflect the translaminar pressure differential between the retrolaminar and intraocular fluid compartments and is a potential biomarker of successful treatment of raised ICP.

This study showed a lack of significant change in pRPE/BM shape measure in the placebo + weight management group, even though the OCT measures of papilledema improved (Figs. 4–7). The explanation for this dissociation is unknown. On one hand, the lack of the ganglion cell layer thinning suggests that the reduction in papilledema was not due to optic atrophy.[8] On the other hand, the persistent BM shape deformation suggests that ICP was still elevated. Thus, the improvement in papilledema raises the possibility that there are non-ICP related mechanisms to reduce swelling, for example an adaptive compensation in axoplasmic flow. Furthermore, the time

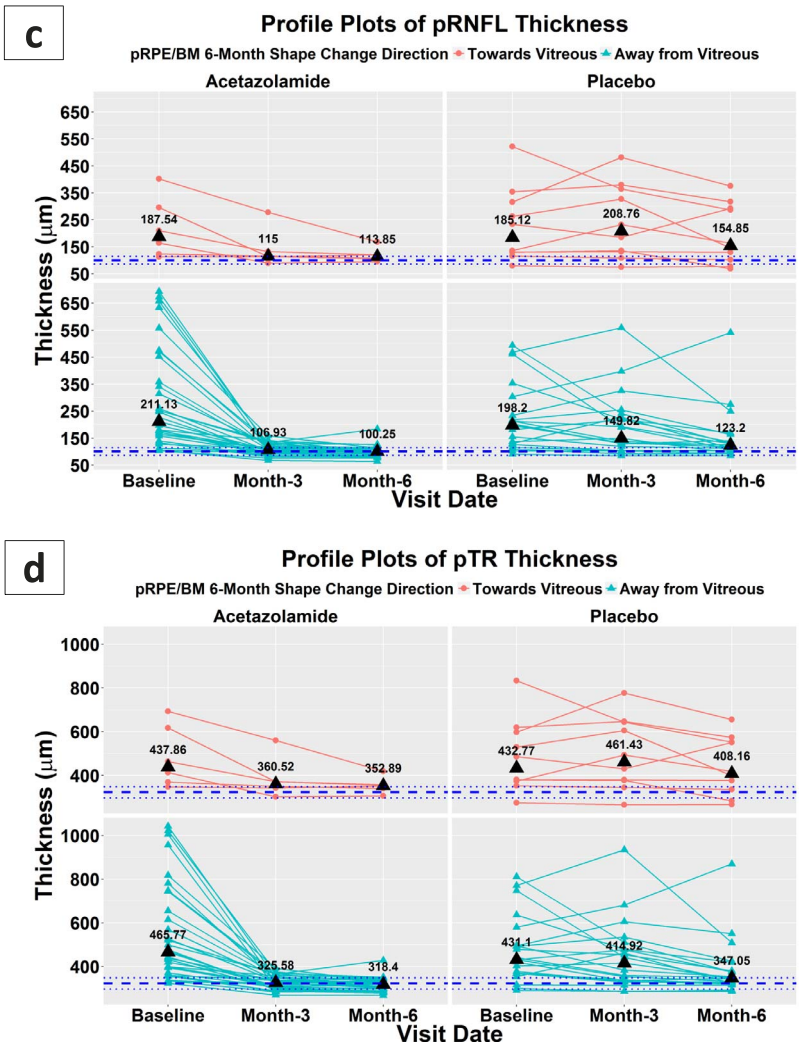

Figure 8. Continued.

course of improvement in the OCT parameters of papilledema was slower, more delayed, and of lesser magnitude in the placebo group compared to the acetazolamide group (Figs. 5–7). Further supporting this possibility is the fact that in the subset of subjects with cerebrospinal fluid (CSF) pressure measurements available at both baseline and 6 months, the reduction in CSF pressure was significantly greater in the acetazolamide group ($P < 0.01$; one-sided unpaired t-test).

It has also been shown that the shape changes associated with ICH are independent of the optic disc edema[10] and take place in patients with optic atrophy where edema is minimal or does not occur.[11] Choroidal folds and flattening of the globe have been reported in patients with ICH who have little or no papilledema.[23,24] Moreover, recent studies have demonstrated that the types and patterns of folds in papilledema, expressions of stress and strain, appears to be a function of two separate but interrelated biomechanical drivers: volumetric expansion of the ONH and anterior deformation of pRPE/BM.[25,26] The specific response to CSF pressure may also be modulated by a variety of individual factors including the geometry and structural stiffness of the scleral flange, dural sheath, and lamina cribrosa and sclera.[25–32]

One challenging aspect of this study was to accurately and consistently place the pRPE/BM opening landmarks on the HD-5LR central B-scans in eyes with severe optic disc swelling. Although HD-5LR scans have higher image quality than the regular SD-OCT volumes, the step of accurately placing landmarks manually is still difficult due to poor OCT signal penetrance in cases where there is more severe optic nerve edema or due to the interference of shadows from more superficial retinal tissue as well as vessels. Figure 9a shows an example where the Bruch's membrane opening region is eclipsed by the shadow from swollen ONH at the nasal side, and Figure 9b gives possible location options for placing the BMO landmark, where the green arrow indicates the decision made in this example. In addition, placing the landmarks at the consistent locations of the BMO instead of the border tissue (e.g., the temporal side in Fig. 9c) is tricky. In this study, the criterion tends to find the ending points of the pRPE/BM surface (i.e., the green arrow in Fig. 9d) rather than the ending points of the border tissue (i.e., the red arrow in Fig. 9d).

Another limitation in this study was the presence of missing data in all the available SD-OCT volumes and HD-5LR raster scans for the overall comparison. Although there were 125 subjects in the original data set, only 39 and 31 subjects in the acetazolamide and placebo groups, respectively, had complete OCT measures at every visit for use in this study (Table 1). Several reasons resulted in the data exclusion including performing wrong OCT exams, incorrectly centered OCT

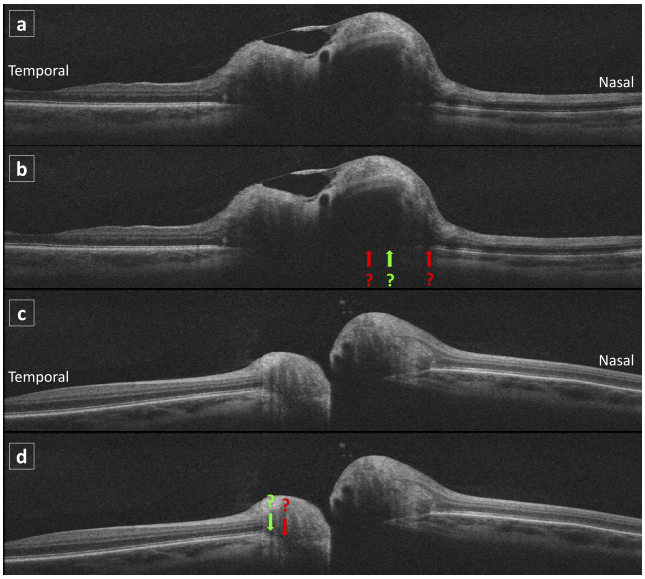

FIGURE 9. Examples of HD-5LR OCT central B-scans showing the difficulties of locating the BMO points: (**a**) the difficulty of the shadow from the swollen optic disc obscuring the opening region, and (**b**) the possible options; (**c**) the difficulty of deciding the end point of the Bruch's membrane instead of the border tissue, and (**d**) the possible options. In both (**b**) and (**d**), the *green arrows* indicate the criteria that was used in this study.

images, truncation of markedly swollen ONH and peripapillary retina, and incomplete data for all three visits.

One future aspect of this work will be to replace the manual step of placing the BMO landmarks with a fully automated analysis. Although the semiautomated method in this study was a significant improvement, reducing the necessary amount of manual landmarks required from 20 landmarks in the traditional manual method[10] to only two landmarks in the semiautomated method,[12] there still exists a need to develop a fully automated method to make the pRPE/BM shape analysis available for data sets without any sample size limitation[33] and without the need for acquiring high density raster scans. Another future direction is to extend the current 2D pRPE/BM shape analysis into a 3D analysis, in which the pRPE/BM opening landmarks are able to be sampled on the entire pRPE/BM surface in an ONH SD-OCT volume rather than just one HD 2D B-scan. A 3D pRPE/SM shape model is expected to have promising advantages because it potentially will have significantly more landmarks than the 2D models have (e.g., hundreds of landmarks in a 3D shape versus 20 landmarks in a 2D shape) and will incorporate 3D contextual information. We also plan to determine whether automated analysis showing pRPE/BM shape changes can accurately reflect the dynamic process occurring at the ONH and reflect changes in CSF pressure from therapy or failed intervention. The hope is that this OCT measure can provide an in vivo noninvasive measure of significant increases or decreases in ICH.

Acknowledgments

A part of this work was presented at the ARVO 2015 annual meeting.

Supported in part by National Institutes of Health Grants U10 EY017281-01A1, U10 EY017387-01A1, 3U10EY017281-01A1S1, R01 EY023279, Unrestricted Grant from Research to Prevent Blindness, C9251-C, Rehabilitation Research & Development (RR&D), Veterans Affairs Office of Research and Development (VA-ORD), Iowa City VA Center for The Prevention and Treatment of Visual Loss.

Disclosure: **J.-K. Wang**, None; **R.H. Kardon**, Novartis (C), Acorda (C), Fight for Sight, Inc. (S), Department of Veteran Affairs Research Foundation (S); **J. Ledolter**, None; **P.A. Sibony**, None; **M.J. Kupersmith**, None; **M.K. Garvin**, P

References

1. Wall M, George D. Idiopathic intracranial hypertension: a perspective study of 50 patients. *Brain*. 1991;114:155–180.
2. Digre KB, Nakamoto BK, Warner JEA, Langeberg WJ, Baggaley SK, Katz BJ. A comparison of idiopathic intracranial hypertension with and without papilledema. *Headache*. 2009;49:185–193.
3. Friedman DI, McDermott MP, Kieburtz K, et al. The idiopathic intracranial hypertension treatment trial: design considerations and methods. *JAMA Neurol*. 2014;34:107–117.
4. Wall M, McDermott MP, Kieburtz KD, et al. Effect of acetazolamide on visual function in patients with idiopathic intracranial hypertension and mild visual loss: the idiopathic intracranial hypertension treatment trial. *JAMA*. 2014;311:1641–1651.
5. Wall M, Kupersmith MJ, Kieburtz KD, et al. The idiopathic intracranial hypertension treatment trial: clinical profile at baseline. *JAMA Neurol*. 2014;74:693–701.
6. OCT Sub-Study Committee for the NORDIC Idiopathic Intracranial Hypertension Study Group. Baseline OCT measurements in the idiopathic intracranial hypertension treatment trial, part I: quality control, comparisons, and variability. *Invest Ophthalmol Vis Sci*. 2014;55:8180–8188.
7. OCT Sub-Study Committee for the NORDIC Idiopathic Intracranial Hypertension Study Group. Baseline OCT measurements in the idiopathic intracranial hypertension treatment trial, part II: correlations and relationship to clinical features. *Invest Ophthalmol Vis Sci*. 2014;55:8173–8179.
8. The Optical Coherence Tomography Substudy Committee and the NORDIC Idiopathic Intracranial Hypertension Study Group. Papilledema outcomes from the optical coherence tomography substudy of the idiopathic intracranial hypertension treatment trial. *Ophthalmology*. 2015;122:1939–1945.
9. Kupersmith MJ, Sibony PA, Mandel G, Durbin M, Kardon RH. Optical coherence tomography of the swollen optic nerve head: deformation of the peripapillary retinal pigment epithelium layer in papilledema. *Invest Ophthalmol Vis Sci*. 2011;52:6558–6564.
10. Sibony PA, Kupersmith MJ, James Rohlf F. Shape analysis of the peripapillary RPE layer in papilledema and ischemic optic neuropathy. *Invest Ophthalmol Vis Sci*. 2011;52:7987–7995.
11. Sibony PA, Kupersmith MJ, Honkanen R, Rohlf FJ, Torab-Parhiz A. Effects of lowering cerebrospinal fluid pressure on the shape of the peripapillary retina in intracranial hypertension. *Invest Ophthalmol Vis Sci*. 2014;55:8223–8231.
12. Wang J-K, Sibony PA, Kardon RH, Kupersmith MJ, Garvin MK. Semi-automated 2D Bruch's membrane shape analysis in papilledema using spectral-domain optical coherence tomography. *SPIE*. 2015;9417:941721.
13. Wall M. Idiopathic intracranial hypertension and the idiopathic intracranial hypertension treatment trial. *J Neuroophthalmol*. 2013;33:1–3.
14. Keltner JL, Johnson C, Cello KE, Wall M. Baseline visual field findings in the idiopathic intracranial hypertension treatment trial (IIHTT). *Invest Ophthalmol Vis Sci*. 2014;55:3200–3207.
15. Li K, Wu X, Chen DZ, Sonka M. Optimal surface segmentation in volumetric images - a graph-theoretic approach. *IEEE Trans Pattern Anal Mach Intell*. 2006;28:119–134.

16. Garvin MK, Abràmoff MD, Wu X, Russell SR, Burns TL, Sonka M. Automated 3-D intraretinal layer segmentation of macular spectral-domain optical coherence tomography images. *IEEE Trans Med Imaging*. 2009;28:1436–1447.
17. Lee K, Niemeijer M, Garvin MK, Kwon YH, Sonka M, Abràmoff MD. Segmentation of the optic disc in 3-D OCT scans of the optic nerve head. *IEEE Trans Med Imaging*. 2010;29:159–168.
18. Wang J-K, Kardon RH, Kupersmith MJ, Garvin MK. Automated quantification of volumetric optic disc swelling in papilledema using spectral-domain optical coherence tomography. *Invest Ophthalmol Vis Sci*. 2012;53:4069–4075.
19. Lawrence MA. Easy analysis and visualization of factorial experiments. 2016. Available at: https://cran.r-project.org/web/packages/ez/ez.pdf.
20. Anand A, Pass A, Urfy MZ, et al. Optical coherence tomography of the optic nerve head detects acute changes in intracranial pressure. *J Clin Neurosci*. 2016;29:73–76.
21. Swanson JW, Aleman TS, Xu W, et al. Evaluation of optical coherence tomography to detect elevated intracranial pressure in children. *JAMA Ophthalmol*. 2017;135:320–328.
22. Brodsky MC, Chen JJ, Wetjen NM. Optical coherence tomography for the noninvasive detection of elevated intracranial pressure: a new role for the ophthalmologist? *JAMA Ophthalmol*. 2017;135:329–330.
23. Griebel SR, Kosmorsky GS. Choroidal folds associated with intreased intracranial pressure. *Am J Ophthalmol*. 2010;129:513–516.
24. Jacobson DM. Intracranial hypertension and the syndrome of acquired hyperopia with choroidal folds. *J Neuroophthalmol*. 1995;15:178–185.
25. Sibony PA, Kupersmith MJ, Feldon SE, Wang J-K, Garvin MK; OCT Sub-Study Committee for the NORDIC Idiopathic Intracranial Hypertension Study Group. Retinal and choroidal folds in papilledema. *Invest Ophthalmol Vis Sci*. 2015;56:5670–5680.
26. Sibony PA, Kupersmith MJ. "Paton's folds" revisited: peripapillary wrinkles, folds, and creases in papilledema. *Ophthalmology*. 2016;123:1397–1399.
27. Downs JC, Roberts MD, Burgoyne CF. Mechanical environment of the optic nerve head in glaucoma. *Optom Vis Sci*. 2008;85:425–435.
28. Burgoyne CF, Crawford Downs J, Bellezza AJ, Francis Suh JK, Hart RT. The optic nerve head as a biomechanical structure: a new paradigm for understanding the role of IOP-related stress and strain in the pathophysiology of glaucomatous optic nerve head damage. *Prog Retin Eye Res*. 2005;24:39–73.
29. Sigal IA, Flanagan JG, Tertinegg I, Ethier CR. Finite element modeling of optic nerve head biomechanics. *Invest Ophthalmol Vis Sci*. 2004;45:4378–4387.
30. Sigal IA, Flanagan JG, Tertinegg I, Ethier CR. Modeling individual-specific human optic nerve head biomechanics. Part I: IOP-induced deformations and influence of geometry. *Biomech Model Mechanobiol*. 2009;8:85–98.
31. Sigal IA, Flanagan JG, Tertinegg I, Ethier CR. Modeling individual-specific human optic nerve head biomechanics. Part II: influence of material properties. *Biomech Model Mechanobiol*. 2009;8:99–109.
32. Sigal IA, Flanagan JG, Ethier CR. Factors influencing optic nerve head biomechanics. *Invest Ophthalmol Vis Sci*. 2005;46:4189–4199.
33. Wang J-K, Kardon RH, Garvin MK. Automated Bruch's membrane opening segmentation in cases of optic disc swelling in combined 2D and 3D SD-OCT images using shape-prior and texture information. In: Chen X, Garvin MK, Liu J, Trucco E, Xu Y, eds. *Proceedings of the Ophthalmic Medical Image Analysis Second International Workshop; Held in Conjunction with MICCAI 2015*; 2015:33–40.

Appendix

OCT Sub-Study Committee for the NORDIC Idiopathic Intracranial Hypertension Study Group

Peggy Auinger, MS (University of Rochester School of Medicine & Dentistry, Rochester, NY, USA), Mary Durbin, PhD (Carl Zeiss Meditec, Inc., Dublin, CA, USA), Steven Feldon, MD, MBA (University of Rochester School of Medicine & Dentistry, Rochester, NY, USA), Mona K. Garvin, PhD (Iowa City VA Health Care System and the University of Iowa, Iowa City, IA, USA), Randy H. Kardon, MD, PhD (Iowa City VA Health Care System and the University of Iowa, Iowa City, IA, USA), John Keltner, MD (University of California, Davis, CA, USA), Mark Kupersmith, MD (OCT Sub-Study Principal Investigator, Icahn School of Medicine at Mount Sinai and New York Eye and Ear Infirmary, New York, NY, USA), Patrick Sibony, MD (State University of New York at Stony Brook, NY, USA), Kim Plumb (University of California, Davis, CA, USA), Jui-Kai Wang, PhD (Iowa City VA Health Care System and the University of Iowa, Iowa City, IA, USA), John S. Werner, PhD (University of California, Davis, CA, USA)

IIHTT Acknowledgment List

Steering Committee: Michael Wall, MD (Principal Investigator, University of Iowa), James Corbett, MD, FAAN (University of Mississippi Medical Center), Steven Feldon, MD, MBA (University of Rochester Eye Institute), Deborah Friedman, MD (UT Southwestern Medical Center), John Keltner, MD (University of California, Davis, CA, USA), Karl Kieburtz, MD, MPH (University of Rochester School of Medicine & Dentistry), Mark Kupersmith, MD (OCT Sub-Study Principal Investigator, Icahn School of Medicine at Mount Sinai and New York Eye and Ear Infirmary, New York, NY, USA), Michael P. McDermott, PhD (University of Rochester School of Medicine & Dentistry), Eleanor B. Schron, PhD, RN, FAAN (Project Officer, National Eye Institute), David Katz, MD (Bethesda Neurology LLC), Tippi Hales (Raleigh Neurology Associates PA), Cindy Casaceli, MBA (University of Rochester School of Medicine & Dentistry)

Sub-Study Sites: New York Eye and Ear Infirmary: Rudrani Banik, MD (Principal Investigator), Sanjay Kedhar, MD (Subinvestigator), Flora Levin, MD (Investigator), Jonathan Feistmann, MD (Investigator), Katy Tai, MA (Coordinator), Alex Yang, BA (Co-coordinator), Karen Tobias, BA (Coordinator), Melissa Rivas, BA (Co-coordinator), Lorena Dominguez, BA (Coordinator), Violete Perez, BA (Coordinator); University of Iowa and Department of Veterans Affairs: Reid Longmuir, MD (Principal Investigator), Matthew Thurtell, MBBS, MSc (Subinvestigator), Trina Eden (Coordinator), Randy Kardon, MD, PhD (Subinvestigator); The Eye Care Group: Robert Lesser, MD (Principal Investigator), Yanina O'Neil, MD (Subinvestigator), Sue Heaton, BS, CCRC (Coordinator), Nathalie Gintowt (Co-coordinator); Bascom Palmer Eye Institute, University of Miami: Byron L. Lam MD (Principal Investigator), Joshua Pasol MD (Subinvestigator), Potyra R. Rosa MD (Coordinator), Alexis Morante MS (Co-coordinator), Jennifer Verriotto MS (Coordinator); Bethesda Neurology, LLC: David Katz, MD (Principal Investigator), Tracy Asbury (Coordinator), Robert Gerwin, MD (Subinvestigator), Mary Barnett (Data Entry); Swedish Medical-Center: Steven Hamilton, MD (Principal Investigator), Caryl Tongco (Coordinator), Beena Gangadharan (Co-coordinator), Eugene May, MD (Subinvestigator); Dean A. McGee Eye Institute: Anil Patel, MD (Principal Investigator), Bradley Farris, MD (Subinvestigator), R. Michael Siatkowsk, MD (Subinvestigator), Heather Miller, LPN (Coordinator), Vanessa Bergman

Investigative Ophthalmology & Visual Science

(Co-coordinator), Kammerin White (Coordinator), Steven O'Dell (Lumbar Puncture), Joseph Andrezik (Lumbar Puncture), Timothy Tytle (Lumbar Puncture); University of Pennsylvania: Kenneth Shindler MD, PhD (Principal Investigator), Joan Dupont (Coordinator), Rebecca Salvo (Coordinator), Sheri Drossner (Co-coordinator), Susan Ward (Coordinator), Jonathan Lo (Coordinator), Stephanie Engelhard (Coordinator), Elizabeth Windsor (Coordinator), Sami Khella (Lumbar Puncture), Madhura Tamhankar, MD (Subinvestigator); Washington University in St. Louis School of Medicine: Gregory Van Stavern, MD (Principal Investigator), Jamie Kambarian (Coordinator), Renee Van Stavern, MD (Subinvestigator), Karen Civitelli (Regulatory), J. Banks Shepherd, MD (Subinvestigator); University of Alabama Birmingham: Michael Vaphiades, DO (Principal Investigator), Jason Swanner, MD (Investigator), A. Blane Jett (Coordinator), Karen Searcey (Coordinator), Frankie Webb (Coordinator), Ashley Knight, BA (Coordinator), Shereka Lewis, BS (Coordinator), Lanning Kline, MD (Subinvestigator), Ronald Braswell, MD (Subinvestigator); Raleigh Neurology Associates, PA: Syndee J. Givre, MD, PhD (Principal Investigator), Tippi Hales (Coordinator), Penni Bye (Coordinator), Keisha Fuller (Coordinator), Kenneth M. Carnes, MD, (Subinvestigator), Kimberly James (Regulatory), Marisol Ragland (Data Entry); Saint Louis University: Sophia M. Chung, MD (Principal Investigator), Dawn M. Govreau, COT (Coordinator), John T. Lind, MD, MS (Subinvestigator); University of Rochester Eye Institute: Zoe Williams, MD (Principal Investigator), George O'Gara (Coordinator), Kari Steinmetz (Coordinator), Mare Perevich (Coordinator), Karen Skrine (Coordinator), Elisabeth Carter (Coordinator), Rajeev Ramchandran, MD (Subinvestigator); Ohio State University: Steven Katz, MD (Principal Investigator), Marc Criden, MD (Investigator), Gina Coman, RMA, CPC, OCS (Co-coordinator), John McGregor, FACS, MD, (Subinvestigator), Andrea Inman (Regulatory); Johns Hopkins University: Prem S. Subramanian, MD, PhD (Principal Investigator), Paul N. Hoffman, MD, PhD (Investigator), Marianne Medura (Coordinator), M. Michaele Hartnett (Coordinator), Madiha Siddiqui (Coordinator), Diane Brown (Coordinator), Ellen Arnold (Co-coordinator), Jeff Boring, MD (Subinvestigator), Neil R. Miller, MD (Subinvestigator); University of Southern California: Peter Quiros, MD (Principal Investigator), Sylvia Ramos (Coordinator), Margaret Padilla (Coordinator), Lupe Cisneros (Coordinator), Anne Kao, MD (Subinvestigator), Carlos Filipe Chicani, MD (Subinvestigator), Kevin Na (Regulatory); University of Houston: Rosa Tang, MD, MPH, MBA (Principal Investigator), Laura Frishman, PhD (Coordinator), Priscilla Cajavilca, MD (Coordinator), Sheree Newland, LVN (Coordinator), Liat Gantz, OD, PhD (Coordinator), Maria Guillermo Prieto, MD (Coordinator), Anastas Pass, OD, JD (Coordinator), Nicky R. Holdeman, OD, MD (Subinvestigator); University of Calgary: William Fletcher, MD, FRCPC (Principal Investigator), Suresh Subramaniam, MSc, MD, FRCPC (Investigator), Jeannie Reimer (Coordinator), Jeri Nickerson (Coordinator), Fiona Costello, MD, FRCPC (Subinvestigator); The Greater Baltimore Medical Center: Vivian Rismondo-Stankovich, MD (Principal Investigator), Maureen Flanagan, CO, COA (Coordinator), Allison Jensen, MD (Subinvestigator); State University of New York at Stony Brook: Patrick Sibony, MD (Principal Investigator), Ann Marie Lavorna, RN (Coordinator), Mary Mladek, COT (Coordinator), Ruth Tenzler, RN (Coordinator), Robert Honkanen, MD (Subinvestigator), Jill Miller-Horn, MD, MS (Lumbar Puncture), Lauren Krupp, MD (Lumbar Puncture); Massachusetts Eye and Ear Infirmary: Joseph Rizzo, MD (Principal Investigator), Dean Cestari, MD (Subinvestigator), Neal Snebold, MD (Investigator), Brian Vatcher (Coordinator), Christine Matera (Coordinator), Edward Miretsky, BA (Coordinator), Judith Oakley, BA (Coordinator), Josyane Dumser (Coordinator), Tim Alperen, BA (Coordinator), Sandra Baptista-Pires (Coordinator), Ursula Bator, OD (Coordinator), Barbara Barrett, RN (Coordinator), Charlene Callahan (Coordinator), Sarah Brett (Coordinator), Kamella Zimmerman (Coordinator), Marcia Grillo (Coordinator), Karen Capaccioli (Coordinator); Duke Eye Center and Duke University Medical Center: M. Tariq Bhatti MD (Principal Investigator), LaToya Greene, COA, CRC (Coordinator), Maria Cecilia Santiago-Turla (Coordinator), Noreen McClain (Coordinator), Mays El-Dairi MD (Subinvestigator); Florida State University College of Medicine: Charles Maitland, MD (Principal Investigator), H. Logan Brooks Jr, MD (Investigator), Ronda Gorsica (Coordinator), Brian Sherman, MD (Subinvestigator), Joel Kramer, MD (Subinvestigator); William Beaumont Hospital: Robert Granadier, MD (Principal Investigator), Tammy Osentoski, RN (Coordinator), Kristi Cumming, RN (Coordinator), Bobbie Lewis, RN (Coordinator), Lori Stec, MD (Subinvestigator)

Dietary Weight Loss Program: Betty Kovacs, Richard Weil, MEd, CDE, Xavier Pi-Sunyer, MD (New York Obesity Nutrition Research Center)

Fundus Reading Center: William Fisher, Dorothea Castillo, Valerie Davis, Lourdes Fagan, Rachel Hollar, Tammy Keenan, Peter MacDowell (University of Rochester Eye Institute)

Visual Reading Field Center: John Keltner, MD, Kim Plumb, Laura Leming, (UC Davis Department of Ophthalmology & Vision Science); Chris Johnson (University of Iowa)

Optical Coherence Tomography Reading Center: John Keltner, MD, John S. Werner, PhD, Kim Plumb, Laura Leming (UC Davis Department of Ophthalmology & Vision Science); Danielle Harvey, PhD (UC Davis Department of Public Health Sciences, Division of Biostatistics)

Data Coordination & Biostatistics Center: Jan Bausch, BS, Shan Gao, MS, Xin Tu, PhD (Biostatistics); Debbie Baker, Deborah Friedman, MD, MPH (Medical Monitor), Karen Helles, Nichole McMullen, Bev Olsen, Larry Preston, Victoria Snively, Ann Stoutenburg (CHET/CTCC) (University of Rochester School of Medicine & Dentistry)

NORDIC Headquarters: O. Iyore Ayanru, Elizabeth-Ann Moss, Pravin Patel (Mount Sinai Roosevelt Hospital) Consultant: Richard Mills, MD (Glaucoma Consultants Northwest)

Data Safety Monitoring Board Members: Maureen Maguire, PhD (Chair, University of Pennsylvania), William Hart Jr, MD, PhD, Joanne Katz, ScD, MS (Johns Hopkins), David Kaufman, DO (Michigan State University), Cynthia McCarthy, DHCE MA, John Selhorst, MD (Saint Louis University School of Medicine)

Adjudication Committee: Kathleen Digre, MD (University of Utah); James Corbett, MD, FAAN (University of Mississippi Medical Center); Neil R. Miller, MD (Johns Hopkins University); Richard Mills, MD (Glaucoma Consultants Northwest)

Investigative Ophthalmology & Visual Science